Materials Research Proceedings 41 (2024) 2190-2199 https://doi.org/10.21741/9781644903131-241

Modelling ductile fracture in an Al alloy with crystal plasticity models

KHADYKO Mikhail[1,2,a*], FRODAL Bjørn Håkon[3] and HOPPERSTAD Odd Sture[2,4]

[1]UiT The Arctic University of Norway, Campus Narvik, Department of Building, Energy and Material Technology, Lodve Langesgate 2, 8514 Narvik, Norway

[2]Centre for Advanced Structural Analysis (CASA), NTNU, Trondheim, Norway

[3]7Waves AS, Slettaveien 21, 1553 Son, Norway

[4]Structural Impact Laboratory (SIMLab), Department of Structural Engineering, NTNU – Norwegian University of Science and Technology, Trondheim, Norway

[a]mikhail.khadyko@uit.no

Keywords: Ductile Fracture, Crystal Plasticity, Finite Element Method, Constituent Particles, Al Alloys

Abstract. Crystal plasticity models enhanced with coupled or uncoupled damage and fracture criteria give an opportunity to account for the role of microstructure in ductile fracture, most directly representing the local variations of stress and strain fields inside and between the grains, voids and particles. Some computationally efficient crystal plasticity, damage and fracture models have recently been developed and applied to some cases of polycrystalline fracture. Such models allow to investigate in a direct way the effects of, e.g., shear bands, larger voids, particles, free surfaces and load direction on the development of damage and fracture. The cast and homogenized Al1.2Mn alloy investigated previously is used here as a basis for simulations. The alloy has an equiaxed grain structure with no texture and contains a population of larger particles and a population of dispersoids. The grain structure and the large particles are modelled directly in the finite element model, while the effect of dispersoids is represented by the damage and fracture part of the single crystal plasticity model. The study investigates the effect of different model parameters and features on the global and local behaviour of the material during localization and fracture, in light of available experimental data.

Introduction

One of the important directions of research in material science is establishing the connection between the macroscopic properties of metal alloys and their microstructure. The multiscale modelling approach considers different length scales from the atomic lattice to crystalline grains, macroscopic structures and components, and aims to predict the behaviour at the larger scale based on the properties at the smaller scale. While the prediction of structural properties based on the fundamental physical laws acting on the atomic lattice level is still out of reach, some more limited studies of the underlying microscopic mechanisms of the macroscopic phenomena may be useful for both predicting and explaining the behaviour of existing materials and for designing new materials.

The present study investigates some aspects of the ductile fracture process in crystalline materials on the scale of the grains and constituent particles, using a combination of well-established methods and theories. The first component to this investigation is the crystal plasticity (CP) theory. The crystal plasticity theory describes a type of plastic deformation in metals as a combination of slips on a set of slip systems [1]. The plastic deformation in polycrystals is heterogeneous on the grain level. This heterogeneity has been experimentally observed, using the digital image correlation (DIC) method [2, 3]. While the slip bands observed in DIC studies [2] cannot yet be reproduced by the CP model, the strain concentrations caused by variation in

crystallographic orientations between the grains can be relatively well predicted by the CP simulations. This ability has been demonstrated in [4] for tantalum oligocrystals and in [5] for copper oligocrystals. The slip activity, i.e., which slip systems are active in which grain, has also been predicted in [5]. Another important aspect of polycrystal plasticity is the appearance of shear bands. Shear band is a type of localization, arising often due to crystallographic softening and can span across multiple grains. The CP models can predict the initiation point and intensity of shear bands in the polycrystals [6, 7].

The second component of the present study is the damage and fracture model. Ductile fracture in metals is known to occur due to nucleation, growth and coalescence of microscopic voids. The plasticity of a material containing voids and their evolution were first modelled in [8, 9]. The Gurson model [8] described the yielding of an isotropic perfect plastic material containing spherical voids. It was later modified to include work-hardening, void coalescence [10], plastic anisotropy [11] and numerous other features. A similar variation of CP model for a crystal containing voids was developed in [12] and implemented and applied in finite element (FE) analyses in [13]. Another less rigorous but more computationally efficient CP model with porosity induced damage was formulated and implemented in [14].

Fracture in metallic materials is an inherently microscopic process. The void size at coalescence and fracture is usually on the micrometre scale and in many cases comparable to the grain size. The voids nucleate at certain parts of the grains due to local stress concentrations and grow in the crystalline medium, which often deforms by plastic slip. Therefore, CP models can be useful in investigating the effects of microstructure features on fracture. Some studies have already been carried out in this direction. In [14, 15] the tensile tests of Al alloys were modelled using a CP model with coupled damage. In [16] the effect of microstructure on ductile fracture in bending was reproduced with the same material model. Other studies include [17], where a CP model with damage was used to study tensile fracture of an olygocrystal, [18], where the CP model was combined with a cohesive zone model, and [19] which implemented a strain-gradient regularization of a porous CP model. Void formation around second phase particles was modelled in [20]. The Fast Fourier Transform solver was used to investigate a polycrystal with non-metallic particles, using a CP model with coupled damage in [21]. The high computational cost of CP models limits either the size of the modelled structure to an oligocrystal or the resolution of the mesh to a few elements per grain, and often 2D plane strain models are used. In addition, the uncertainty in the microscopic material parameters make the results mostly valid in the qualitative sense. Nevertheless, these studies may become a valuable supplement to the other experimental and numerical methods of investigating fracture.

In the present work some aspects of modelling the ductile fracture in polycrystalline materials is investigated with CP models with coupled damage. An experimental study of the cast and homogenized Al1.2Mn alloy [22] is used as the basis for modelling. The microstructure of the alloy including the grain morphology, the crystallographic texture and the constituent particles, is reproduced in a 2D FE model. The constituent particles are explicitly modelled as elastic inclusions, which fracture at a given level of the von Mises stress, creating voids, whereas previous studies usually only introduced the already existing voids [23]. The coupled damage CP model is used to account for the dispersoids in the Al1.2Mn alloy and their contribution to the ductile fracture. The study investigates the onset and development of localization and ductile fracture for a microstructure containing constituent particles with different strength. The simulations show a complex interaction between the grain boundaries, the voids, the shear bands and the ductile crack and the influence of the two different particle populations on ductile fracture.

Finite element model

The Al1.2Mn alloy [22] is used as a reference to create the microstructure model. The alloy is in the cast and homogenized condition and consists of equiaxed grains with an average diameter of 60 μm with no texture. The constituent particles are predominantly distributed along the grain and dendrite boundaries and are mostly rounded, with a low number of elongated particles. The grain morphology and particle distribution may be seen in Fig. 1. The area fraction of the particles is 2.4 %, with a mean maximum length of 1.1 μm and a standard deviation of 1.2 μm. The alloy also contains a large number of dispersoids with diameter below 1 μm. The numerical model, created in the Abaqus FEA software, reproduces these essential features of the microstructure. The Neper software is used to generate a 450 × 450 μm tessellation, containing 50 grains, based on a grain growth algorithm [24], corresponding to an average grain diameter of 60 μm. The spherical particles with diameter of 2 μm are evenly distributed along the grain boundaries at 8 μm distance from each other, so that the area fraction is approximately 2.4 %. Due to uncertainty in size and area fraction of the dendrite particles, they are not represented in the model. The model is shown alongside the microstructure in Fig. 1. The model is a 2D representation of the material, with plane strain boundary conditions. The left edge of the model is fixed and the right one is moving with a speed smoothly ramped up to a constant value, simulating plane strain tension.

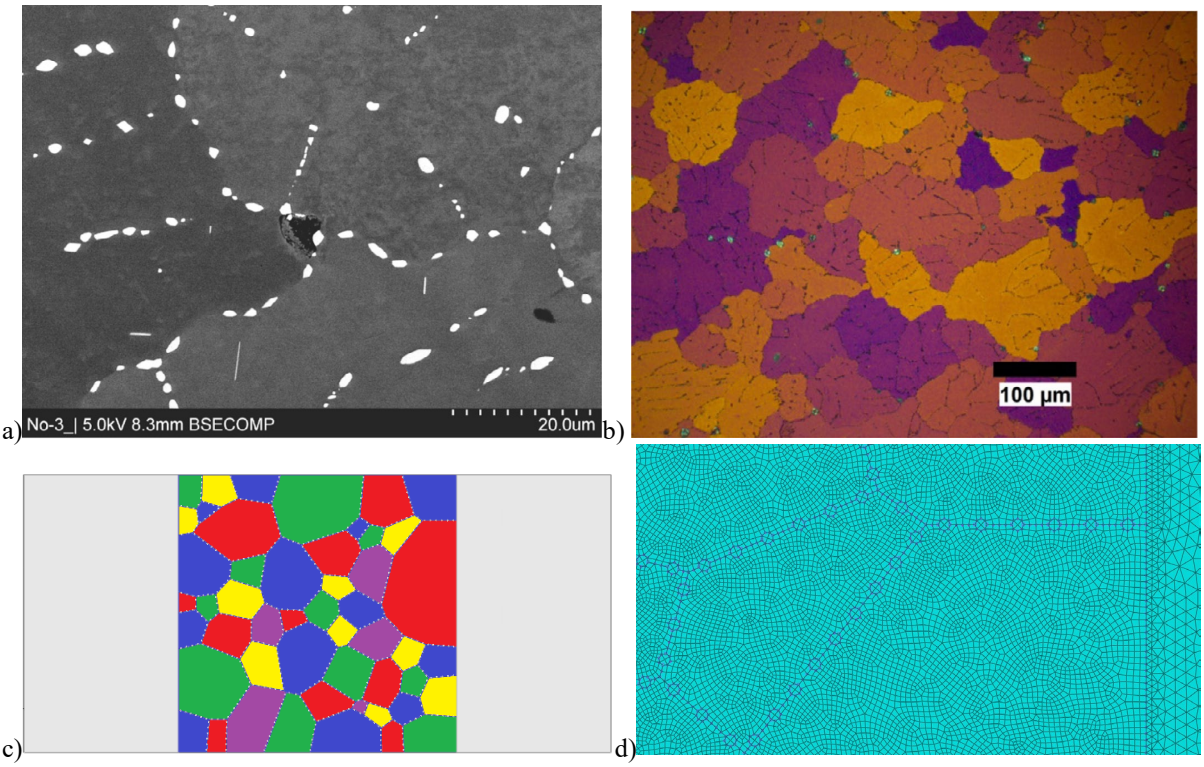

Figure 1. The microstructure of Al1.2Mn alloy: a) constitutive particle size and distribution, b) grain morphology, c) numerical model with 50 grains in the centre and the isotropic plasticity boundary layers on the sides, marked by grey colour d) element mesh near the boundary layer.

The coupled damage CP model is implemented as an Abaqus FEA user-defined material model, as described in [14]. The plastic flow is described by a rate-dependent constitutive relation:

$$\dot{\gamma}^{\alpha} = \dot{\gamma}_0 \left| \frac{\tau^{(\alpha)}}{(1-\omega)\tau_c^{(\alpha)}} \right|^{\frac{1}{m}} sgn\left(\tau^{(\alpha)}\right), \quad (1)$$

where $\dot{\gamma}^{\alpha}$ is the slip rate on slip system α, $\dot{\gamma}_0$ is the reference slip rate, m is the instantaneous rate sensitivity parameter, $\tau^{(\alpha)}$ is the resolved shear stress, $\tau_c^{(\alpha)}$ is the critical resolved shear stress and

ω is the damage parameter. The critical resolved shear stress evolution is described by the Voce type equation:

$$\dot{\tau}_c^{(\alpha)} = \sum_{\beta=1}^{N} \sum_{k=1}^{2} \theta_k \exp\left(-\frac{\theta_k}{\tau_k}\Gamma\right) q_{\alpha\beta}, \quad (2)$$

where $q_{\alpha\beta}$ is the latent hardening matrix, θ_k and τ_k are the hardening parameters and Γ is the accumulated plastic shear strain. The initial value of critical resolved shear stress is denoted as τ_0. The damage evolution is described by equation:

$$\dot{\omega} = \frac{3}{4} q_1 q_2 \omega(1-\omega) \sinh\left(\frac{3}{2} q_2 T\right) \dot{\Gamma}, \quad (3)$$

where q_1 and q_2 are the damage parameters and T is the stress triaxiality ratio. The initial and critical values of the damage parameter are denoted ω_0 and ω_c. The elastic constants, rate sensitivity, reference slip rate and latent hardening parameter are taken from [14]. The critical slip and work hardening parameters are obtained by fitting the slip system resistance equation multiplied by the Taylor factor equal to 3 (approximately corresponding to the notexture value) to the equivalent stress-strain curve of the alloy taken from [22]. The result is approximate, but considering the nature of the study it is sufficient to represent the alloys work hardening behaviour and as demonstrated in [25] the local strain distribution and localization are not overly sensitive to the work hardening parameters. The parameters used in the study are given in Table 1.

Table 1: Parameters of the CP model.

τ_0[MPa]	θ_1[MPa]	τ_1[MPa]	θ_2[MPa]	τ_2[MPa]	ω_0	ω_c	q_1	q_2
13.0	191.0	16.5	24.0	34.0	0.006	0.12	1.5	1.0

A set of 50 random crystallographic orientations was assigned to the 50 grains of the FE model. The left and right boundary layers of the model, indicated by grey colour in Fig. 1 are assigned an isotropic elastic-plastic material with the same equivalent stress-strain curve. This creates a more natural and relaxed boundary at the edges and forces localization in the central part of the model, avoiding necking and shear bands at the fixed edges. The particles are assigned an isotropic elastic material with Young's modulus equal to 210 GPa and Poisson's ratio equal to 0.3.

The fracture model parameters for the coupled damage CP model are taken from [14], where it was calibrated for the population of constituent particles in the cast and homogenized AA6063 alloy. Considering that both Al alloys are cast and homogenized, the effect of dispersoids and constituent particles on fracture in the Al1.2Mn alloy is practically impossible to separate, and the study is largely qualitative in nature, no further adjustments were made to the fracture parameters. The constituent particles are assigned a separate simple fracture criterion. When the von Mises stress in the particle reaches a certain threshold value, the corresponding element is eroded. The threshold stress is one of the parameters that were investigated in the study. It was assigned several increasing values: 100 MPa for what is later referred to as "weak particles", 500 MPa for "medium strength particles", 1000 MPa for "strong particles" and a very large value for "elastic particles". The threshold stress may be interpreted as either the strength of the particles themselves or the particle-matrix interface.

The size of the modelled microstructure was chosen based on computational limitations. The mesh resolution should allow for representing the particles by at least several elements, while maintaining a similar element size for the whole oligocrystal model. Using a finer mesh around the particles or grain boundaries (GBs) and a coarser mesh inside the grains was found to affect the localization and fracture, thus a homogeneous element size was used. At the same time the total number of elements should not be too large, making the FE simulation time unfeasibly long. The additional limitation is that the simulation is run until global fracture or until some instability arises in the most deformed element, which for a ductile Al1.2Mn alloy leads to a large final global displacement and increased computation time. The resulting model and the corresponding mesh

are shown in Fig. 1. The mesh of the oligocrystal part contains 120 000 linear hexahedral fully integrated elements, same type as used in [14]. The boundary layers of the model were meshed with 3000 wedge type elements. The simulations were run with the Abaqus/Explicit solver. Mass-scaling was applied to decrease the computation time and the kinetic energy was controlled at every step to ensure that it was small compared to the total energy and that the simulation remained quasi-static. The simulation time until fracture was around 5-7 days on 8 cores of a computer cluster node.

To investigate the effect of particles on the fracture simulations, the following variations were tested. Firstly, simulations with the CP model without damage were run. A baseline model contained no particles, then the same oligocrystal, but with elastic, strong, medium, and weak particles was simulated. Secondly, the coupled damage CP simulations were run, with a baseline oligocrystal and then the oligocrystal with particles. Several different oligocrystal morphologies and random orientation sets were tested, but they all yielded the same trends, so only one is shown further.

Results and discussion

The contours of the von Mises equivalent plastic strain for the simulations with the CP model are presented in Fig. 2. The baseline simulation shows a typical shear band type localization, originating in softer grains with favourable orientations and propagating through the whole model. The introduction of elastic particles does not significantly affect the results and the same localization band arises, although with slightly reduced intensity. When strong particles (with a finite although high strength) are introduced, large strains in the shear band and the corresponding stress concentrations manage to erode some of the particles, thus creating a softer material locally and increasing the localization intensity. Decreasing the particle strength further leads to faster erosion of particles at the GBs with the highest stress concentrations, producing a large soft zone and concentrating the strain there, interrupting further concentration in the shear band. The weak particles quickly erode, leaving a crystal with voids. The result is strain concentration around the growing voids, which prevents the shear band from propagating out of the weaker grain where it originated. Instead, the voids grow quickly at several favourably oriented (normal to tensile direction) GBs on softer grains, leading to a quick softening effect of the global force-displacement curve. Fig. 3 shows contour plots of the equivalent plastic strain at the end of the simulations with the coupled damage CP model. Fracture occurs first in the shear band, but after initiation it does not propagate along the band, it follows its own path instead. The ductile crack propagation may be traced more clearly in Fig. 4, which shows plots of the damage distribution at the end of the simulations. The fracture may initiate and propagate either through softer grains with large plastic strains, or along the GBs due to higher stress concentrations. The introduction of elastic particles changes the fracture development. Additional stress concentrations around the particles lead to earlier fracture in the crystal, more concentrated damage, and a change of the crack propagation path.

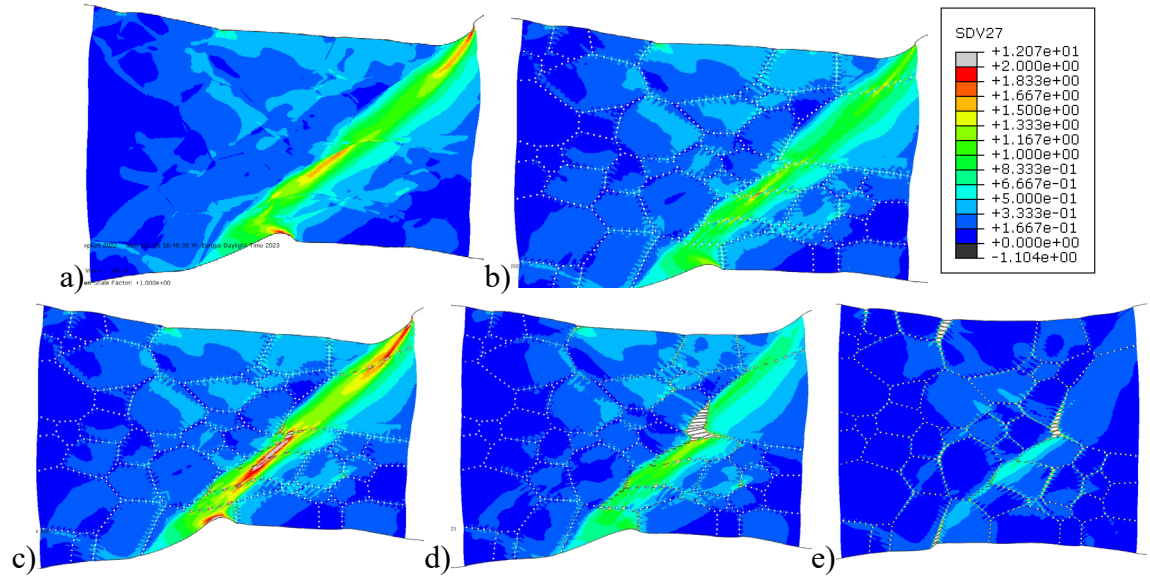

Figure 2: Equivalent plastic strain contours for the CP model at the end of the simulation for: a) baseline oligocrystal, b) model with elastic particles, c) model with strong particles, d) model with medium particles, and e) model with weak particles.

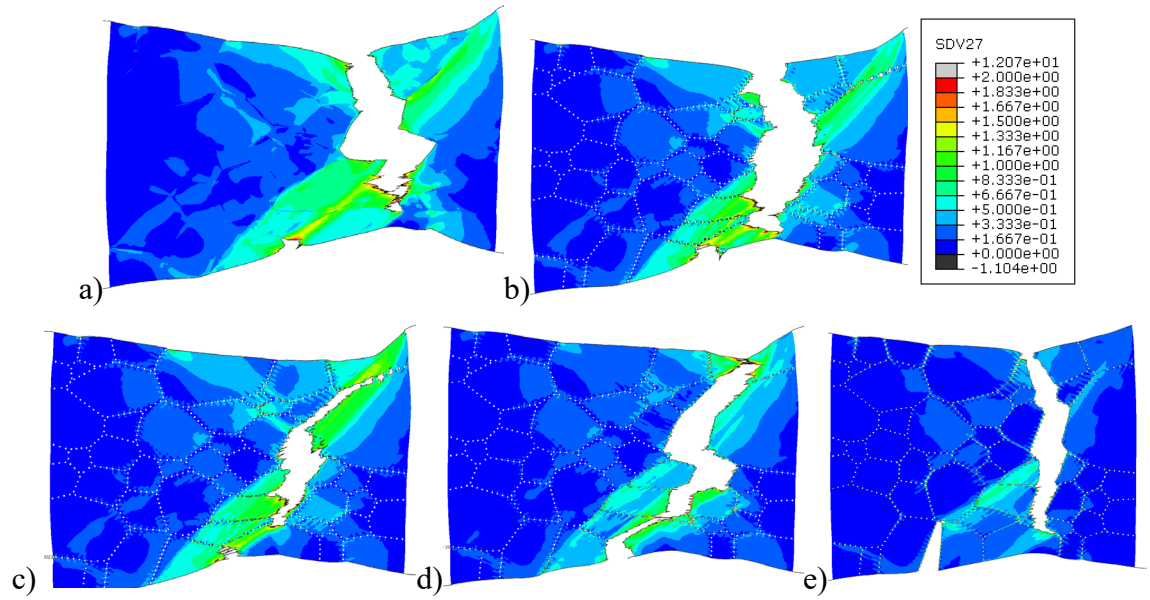

Figure 3: Equivalent plastic strain contours for the coupled damage CP model at the end of simulation for: a) baseline oligocrystal, b) model with elastic particles, c) model with strong particles, d) model with medium particles, and e) model with weak particles.

As the particle strength is decreased, some of the particles get eroded and produce voids. The voids lead to a combination of stress concentrations and large plastic strains, as they grow, which enhances the damage development in the crystal around them. As a result, strain and damage tend to concentrate more and more on the GBs around the particles and voids. The damage variable is more dispersed inside the grains in the simulations with no particles and elastic particles, while in the simulations with medium and weak particles the damage is extremely concentrated in the GB zone. Nevertheless, even in the simulation with weak particles, some transgranular fracture occurs, with certain combinations of softer grains and GB orientations. It is observed that two grains are fractured through the thickness by the ductile crack, with a very concentrated damage field around it.

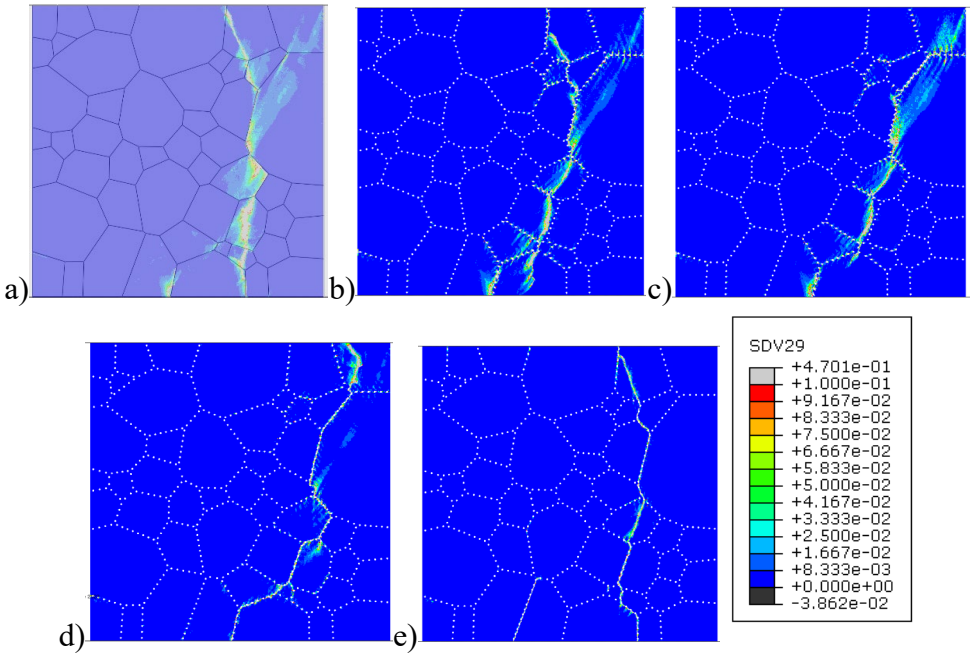

Figure 4: Damage variable for the coupled damage CP model at the end of simulation on the undeformed configuration for: a) baseline oligocrystal, b) model with elastic particles, c) model with strong particles, d) model with medium particles, and e) model with weak particles.

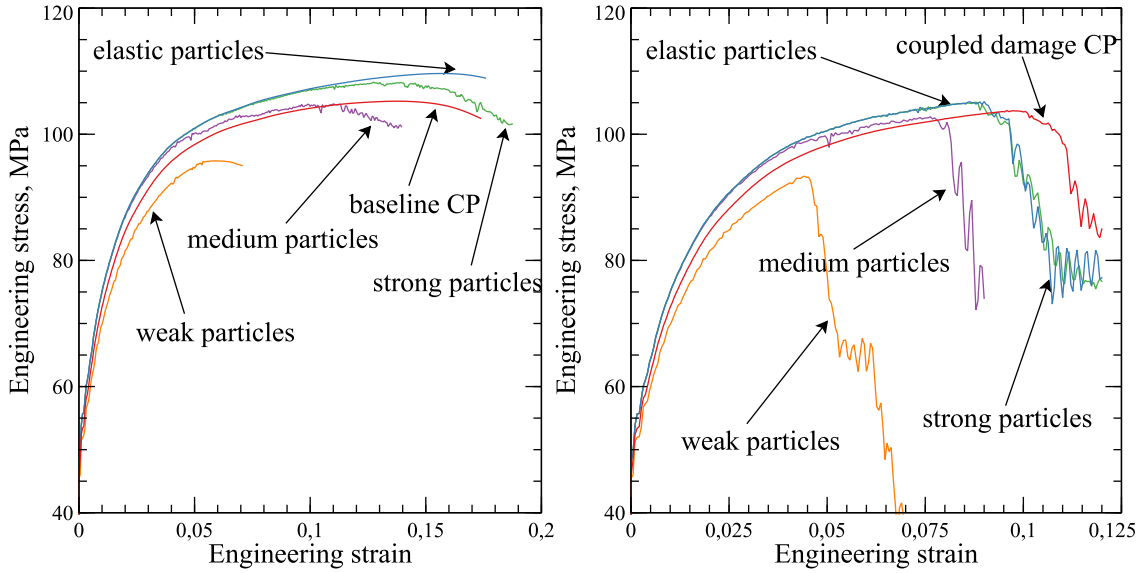

Figure 5: Engineering stress-strain curves obtained from the simulations with the CP model on the left and the coupled damage CP model on the right.

The engineering stress-strain curves for the simulations are presented in Fig. 5. In the baseline case of no damage in the CP model, the introduction of elastic particles just reinforces the material. The point at which the strong particles begin to erode may be identified on the stress-strain curve by the onset of softening. Comparing the curves for different particle strength it may be seen that the strain at which the material begins to soften is approximately proportional to the particle strength. A similar trend is observed in the simulations with the coupled damage CP model, although the stress reduction is much more abrupt. The results show that the effect of particle strength on the stress-strain curve and damage is quite significant and cannot be neglected, e.g., when fitting the work hardening and damage parameters of the CP model.

The fractography of the Al1.2Mn in [22] shows two populations of dimples, coarse and fine, with coarse dimples often containing constituent particles. This is interpreted in [22] as the evidence for coarse dimples originating on the constituent particles and correspondingly the fine ones on the dispersoids. The simulations show that the proportion of coarse dimples in the ductile crack can be correlated, among other things with the particle strength or the particle-matrix interface strength. The longitudinal cross-section of the fracture zone in [22] also may be used to evaluate how much void formation occurred in the vicinity of the ductile crack and compare it to the simulation results, which show a significant variation in the damage distribution, depending on the particle strength.

The most prominent aspect of the simulations is the critical role of localization in the response of the material. The strain localizes either due to crystallographic softening or void growth and coalescence, showing quite distinct distributions of strain and damage in the two cases, which transform one into the other as the particle strength decreases. The shear bands tend to be oriented at approximately a 45-degree angle to the tensile axis, while for the case of weak particles the localization is dominated by the zones around the GBs normal to the tensile axis. The orientation of the fracture surface from the experiments may be compared to the orientation of the fracture surface from the simulations.

Conclusions

The ductile fracture in the Al1.2Mn alloy was modelled using a 2D FE model with a coupled damage CP model for the grains and an elastic model for the particles. The qualitative effect of particles, their strength and the presence of a second population of smaller particles were investigated. The threshold stress for particle fracture had a pronounced effect on the stress-strain curve, the type and intensity of the localization in the material, the distribution of damage in the coupled damage CP model, the proportion of fracture in the coarse and fine particles, and the path of the ductile crack through the material. These results may be compared to the experimentally observed features of ductile fracture in the Al1.2Mn alloy.

References

[1] R. J. Asaro, "Crystal plasticity," *J Appl Mech,* 50 (1983) 921-934. https://doi.org/10.1115/1.3167205

[2] F. Di Gioacchino and J. Q. da Fonseca, "An experimental study of the polycrystalline plasticity of austenitic stainless steel,"*Int J Plasticity,* 74 (2015) 92-109. https://doi.org/10.1016/j.ijplas.2015.05.012

[3] A. Guery, F. Hild, F. Latourte, and S. Roux, "Slip activities in polycrystals determined by coupling DIC measurements with crystal plasticity calculations," *Int J Plasticity,* 81 (2016) 249-266. https://doi.org/10.1016/j.ijplas.2016.01.008

[4] H. Lim, J. D. Carroll, C. C. Battaile, B. L. Boyce, and C. R. Weinberger, "Quantitative comparison between experimental measurements and CP-FEM predictions of plastic deformation in a tantalum oligocrystal," *Int J Mech Sci,* vol. 92, pp. 98-108, 2015. https://doi.org/10.1016/j.ijmecsci.2014.12.010

[5] D. Depriester, J. Goulmy, and L. Barrallier, "Crystal Plasticity simulations of in situ tensile tests: A two-step inverse method for identification of CP parameters, and assessment of CPFEM capabilities," *Int J Plasticity,* 168 (2023)103695. https://doi.org/10.1016/j.ijplas.2023.103695

[6] T. F. Morgeneyer *et al.*, "On crystallographic aspects of heterogeneous plastic flow during ductile tearing: 3D measurements and crystal plasticity simulations for AA7075-T651," *Int J Plasticity,* 144 (2021) 103028. https://doi.org/10.1016/j.ijplas.2021.103028

[7] K. M. Min, H. Lee, H.-D. Joo, H. N. Han, and M.-G. Lee, "Crystal Plasticity Simulation of Shear Band Formation and Recrystallization Texture in Grain-Oriented Electrical Steel," *Available at SSRN 4467215*.

[8] A. L. Gurson, "Continuum theory of ductile rupture by void nucleation and growth: Part I—Yield criteria and flow rules for porous ductile media," *J Eng Mater,* 99 (1977) 2-15. https://doi.org/10.1115/1.3443401

[9] J. R. Rice and D. M. Tracey, "On the ductile enlargement of voids in triaxial stress fields," *J Mech Phys Solids,* 17 (1969) 201-217. https://doi.org/10.1016/0022-5096(69)90033-7

[10] V. Tvergaard and A. Needleman, "Analysis of the cup-cone fracture in a round tensile bar," *Acta Metall Mater,* 32 (1984) 157-169. https://doi.org/10.1016/0001-6160(84)90213-X

[11] L. E. B. Dæhli, J. Faleskog, T. Børvik, and O. S. Hopperstad, "Unit cell simulations and porous plasticity modelling for strongly anisotropic FCC metals," *Eur J Mech A-Solid,* 65 (2017) 360-383. https://doi.org/10.1016/j.euromechsol.2017.05.004

[12] X. Han, J. Besson, S. Forest, B. Tanguy, and S. Bugat, "A yield function for single crystals containing voids," *Int. J Solids Struct,* 50 (2013) 2115-2131. https://doi.org/10.1016/j.ijsolstr.2013.02.005

[13] M. Khadyko, B. H. Frodal, and O. S. Hopperstad, "Finite element simulation of ductile fracture in polycrystalline materials using a regularized porous crystal plasticity model," *International Journal of Fracture,* 228 (2021) 15-31. https://doi.org/10.1007/s10704-020-00503-w

[14] B. H. Frodal, S. Thomesen, T. Børvik, and O. S. Hopperstad, "On the coupling of damage and single crystal plasticity for ductile polycrystalline materials," *Int J Plasticity,* 142 (2021) 102996. https://doi.org/10.1016/j.ijplas.2021.102996

[15] A. Li, W. Hu, H. Li, Z. Zhan, and Q. Meng, "A crystal plasticity-based microdamage model and its application on the tensile failure process analysis of 7075 aluminum alloy," *Mat Sci Eng,* 884 2023) 145541. https://doi.org/10.1016/j.msea.2023.145541

[16] B. H. Frodal, L. Lodgaard, Y. Langsrud, T. Børvik, and O. S. Hopperstad, "Influence of Local Microstructural Variations on the Bendability of Aluminum Extrusions: Experiments and Crystal Plasticity Analyses," *J Appl Mech,* 90 (2023) 041006. https://doi.org/10.1115/1.4056429

[17] C. K. Cocke *et al.*, "Implementation and experimental validation of nonlocal damage in a large-strain elasto-viscoplastic FFT-based framework for predicting ductile fracture in 3D polycrystalline materials,"*Int J Plasticity,* 162 (2023) 103508. https://doi.org/10.1016/j.ijplas.2022.103508

[18] T. Yalçinkaya, İ. T. Tandoğan, and İ. Özdemir, "Void growth based inter-granular ductile fracture in strain gradient polycrystalline plasticity," *Int J Plasticity,* 147 (2021) 103123. https://doi.org/10.1016/j.ijplas.2021.103123

[19] J.-M. Scherer, J. Besson, S. Forest, J. Hure, and B. Tanguy, "A strain gradient plasticity model of porous single crystal ductile fracture,"*J Mech Phys Solids,* 156 (2021) 104606. https://doi.org/10.1016/j.jmps.2021.104606

[20] P. Gao, M. Fei, M. Zhan, and M. Fu, "Microstructure-and damage-nucleation-based crystal plasticity finite element modeling for the nucleation of multi-type voids during plastic deformation of Al alloys," *Int J Plasticity,* 165 (2023) 103609. https://doi.org/10.1016/j.ijplas.2023.103609

[21] F. Qayyum *et al.*, "Influence of non-metallic inclusions on local deformation and damage behavior of modified 16MnCrS5 steel," *Crystals,*12 (2022) 281. https://doi.org/10.3390/cryst12020281

[22] I. Westermann, K. O. Pedersen, T. Furu, T. Børvik, and O. S. Hopperstad, "Effects of particles and solutes on strength, work-hardening and ductile fracture of aluminium alloys,"*Mechanics of Materials,* 79 (2014) 58-72. https://doi.org/10.1016/j.mechmat.2014.08.006

[23] J. Liu, Z. Li, M. Huang, J. Zhu, L. Zhao, and Y. Zhu, "Crystallographic texture effect on statistical microvoid growth in heterogeneous polycrystals," *Int. J Solids Struct,* 281 (2023) 112435. https://doi.org/10.1016/j.ijsolstr.2023.112435

[24] R. Quey and M. Kasemer, "The neper/fepx project: free/open-source polycrystal generation, deformation simulation, and post-processing," in *IOP Conference Series: Materials Science and Engineering*, 2022, vol. 1249, no. 1: IOP Publishing, p. 012021. https://doi.org/10.1088/1757-899X/1249/1/012021

[25] M. Khadyko, J. Sturdy, S. Dumoulin, L. R. Hellevik, and O. S. Hopperstad, "Uncertainty quantification and sensitivity analysis of material parameters in crystal plasticity finite element models,"*Journal of Mechanics of Materials and Structures,* 13 (2018) 379-400. https://doi.org/10.2140/jomms.2018.13.379